Published in final edited form as:
J Immunol. 2009 December 1; 183(11): 7489–7496. doi:10.4049/jimmunol.0901414.

The Oxazolidinone Derivative Locostatin Induces Cytokine Appeasement[1]

Antoine Ménoret[*], **Jeremy P. McAleer**[*], **Soo-Mun Ngoi**[*], **Swagatam Ray**[†], **Nicholas A. Eddy**[‡], **Gabriel Fenteany**[‡], **Seung-Joo Lee**[*], **Robert J. Rossi**[*], **Bijay Mukherji**[†], **David L. Allen**[§], **Nitya G. Chakraborty**[†], and **Anthony T. Vella**[*,2]

[*] Department of Immunology, University of Connecticut Health Center, Farmington, CT 06032

[†] Department of Medicine, University of Connecticut Health Center, Farmington, CT 06032

[‡] Department of Chemistry, University of Connecticut, Storrs, CT 06269

[§] NextGen Sciences Inc, Ann Arbor, MI 48108

Abstract

Damaging inflammation arising from autoimmune pathology and septic responses results in severe cases of disease. In both instances, anti-inflammatory compounds are used to limit the excessive or deregulated cytokine responses. We used a model of robust T cell stimulation to identify new proteins involved in triggering a cytokine storm. A comparative proteomic mining approach revealed the differential mapping of Raf kinase inhibitory protein after T cell recall in vivo. Treatment with locostatin, an Raf kinase inhibitory protein inhibitor, induced T cell anergy by blocking cytokine production after Ag recall. This was associated with a reduction in Erk phosphorylation. Importantly, in vivo treatment with locostatin profoundly inhibited TNF-α production upon triggering the Ag-specific T cells. This effect was not limited to a murine model because locostatin efficiently inhibited cytokine secretion by human lymphocytes. Therefore, locostatin should be a useful therapeutic to control inflammation, sepsis, and autoimmune diseases.

Recognition of peptide MHC by the TCR is the key step initiating T cell activation. However, in the absence of costimulation, TCR engagement depletes a T cell's capacity to synthesize IL-2, fostering a state of Ag-specific anergy (1,2). In addition, the immune system contains other mechanisms of peripheral T cell tolerance, including a network of regulatory T cells to modulate and down-regulate proinflammatory immune responses (3). Although regulatory T cells extrinsically regulate effector T cells through cytokine deprivation (4), T cell anergy directly affects the intrinsic signaling pathways of Ag-specific T cells (5). Therefore, coupled with emerging knowledge of the specific antigenic triggers responsible for various immune pathologies, induction of T cell anergy presents a direct therapeutic goal for the treatment of autoimmune disorders, septic shock, transplant rejection, and exacerbated infectious diseases. Current drugs that can induce T cell anergy, like the immunophilin ligands cyclosporine A, FK-506, rapamycin, and sanglifehrin A, are useful in this approach (6). However, new compounds that induce T cell anergy and inhibit TLR stimulation, which also causes

[1]This work was supported by University of Connecticut Health Center Start-up Funds, National Institutes of Health Grants AI 52108 and AI 42858 (to A.T.V.) and GM077622 (to G.F.).

2Address correspondence and reprint requests to Dr. Anthony T. Vella, Department of Immunology-MC1319, University of Connecticut Health Center, 263 Farmington Avenue, Farmington, CT 06032. vella@uchc.edu.

Disclosures
The authors have no financial conflict of interest.

immunopathology, would provide a significant and distinct therapeutic advantage and enhance patient safety.

One approach to discover new targets for immune regulation relies on differentially identifying signaling proteins regulated during effector T cell stimulation. A proteomic differential screening approach offers a number of advantages, including the ability to detect changes in protein expression, modification, and interactions. We developed an in vivo T cell stimulation model that results in cytokine release rivaling responses produced by LPS stimulation. In vivo peptide challenge causes robust T cell dependant IFN-γ and TNF-α release into the serum. Taking advantage of this model (7,8), we used a proteomic-based method (9) to differentially compare the resting to stimulated state. Our results show that Raf kinase inhibitor protein (RKIP),[3] also known as phosphatidylethanolamine-binding protein, is uniquely localized on the proteomic map after induction of the cytokine storm. Based on these data, we hypothesized that a specific inhibitor called locostatin would induce T cell anergy, and our data demonstrate a powerful reduction of effector cytokine release upon T cell recall. Mechanistically, we demonstrate that after TCR triggering, locostatin uncouples Erk phosphorylation in primed but not naive cells. Finally, and perhaps more importantly, when tested against human PBMC for its cytokine appeasement capacity, locostatin blocked TCR and LPS-induced cytokine production. We conclude that locostatin therapy may doubly target T cell responses during autoimmunity and TLR stimulation as manifested during septicemia.

Materials and Methods

Mice, cells, and Abs

C57BL/6 mice were purchased from the National Cancer Institute or The Jackson Laboratory. OT-I mice (10) were bred at the University of Connecticut Health Center and all mice were maintained under pathogen-free conditions and handled in accordance to National Institutes of Health federal guidelines. HLA-A2-positive healthy normal donors were included in the study population with informed consent (Dr. Bijay Mukherji, University of Connecticut Health Center). T2 cell-line was a gift to Dr. Mukherji from Dr. S. Rosenberg (Surgery Branch, National Cancer Institute, Bethesda, MD) and the agonist anti-CD137 mAb was purified from 3H3 hybridoma culture supernatant (a gift from Dr. Robert Mittler, Emory University; Atlanta, GA; Ref. 11). Anti-IFN-γ-PE and TNF-α ELISA kits were purchased from BD Pharmingen. Anti-TNF-α-allophycocyanin and anti-CD45.1-FITC were purchased from eBioscience. Anti Erk, p-Erk, and RKIP Abs were purchased from Cell Signaling Technology. The specificity of the anti-RKIP Ab was verified using RKIP knockout mouse spleen and liver provided by Dr. Jan Klysik, Brown University, Rhode Island (12).

Chemicals

Disulfiram (aldehyde dehydrogenase and NFκB inhibitor) and ethacrynic acid (glutathione S-transferase inhibitor) were purchased from Sigma-Aldrich. Z-Pro-Pro-CHO (prolyl oligopeptidase inhibitor) was purchased from BIOMOL. Locostatin (RKIP inhibitor) was synthesized in the Fenteany laboratory as previously published (13), and also purchased from Calbiochem; both preparations of locostatin performed identically. The four inhibitors above were solubilized in DMSO at a final concentration of 50 mM, aliquoted, and stored at −20°C before use. DMSO was used as vehicle control in all experiments. All other chemicals were purchased from Sigma-Aldrich.

[3]Abbreviations used in this paper: RKIP, Raf kinase inhibitor protein; pI, protein isoelectric point; DC, dendritic cell; MALDI-TOF, matrix-assister laser desorption/ionisation time of flight; LC/MS/MS, Liquid chromatography-tandem mass spectrometry.

Cell processing and PF 2D proteomics

We i.v. transferred ~1.5×10^5 OT-I cells into C57BL/6 mice, and a day later, mice were i.p. injected with OVA (1 mg), anti-CD137 (3H3 mAb at 50–100 μg), and poly IC (150 μg). On day 6 after immunization, mice were i.p. injected with 0.1 mg SIINFEKL or vehicle. After 3 h, spleens and peripheral lymph nodes were crushed through nylon mesh cell strainers (BD Biosciences), RBC lysed with ammonium chloride solution (155 mM NH_4Cl, 10 mM $KHCO_3$, (pH 7.2)), and cells were enumerated using a Z1 particle counter (Beckman Coulter). Cells were washed once in cold PBS and stored at −80°C as a dried pellet. Cell lysis was performed with lysis buffer (7.5 M urea, 2.5 M thiourea, 12.5% glycerol, 62.5 mM Tris-HCl, 2.5% n-octyl β-D-glucopyranoside, 6.25 mM TCEP, 1.25 mM protease inhibitor mixture (Sigma-Aldrich no. P2714)). Lysates were centrifuged at 25,000 × *g* for 1 h at 18°C. The buffer of the supernatant was exchanged using PD-10 columns (Sigma-Aldrich) pre-equilibrated with PF 2D start buffer (Beckman Coulter no. 391110). The resulting sample was quantified by Micro BCA Protein Assay Kit (Pierce no. 23235), diluted in PF 2D start buffer and loaded on a Beckman Coulter ProteomeLab PF 2D platform, as described before (9). Fractions corresponding to the linear gradient between pH 8.0 through 4.0 were further separated on a HPRP column (Beckman Coulter no. 391106) through an automated autoloader. A gradient was run from 0 to 100% of acetonitrile and 0.085% trifluoroacetic acid on a HPRP column at 50°C. The proteins were detected with UV light at 214 nm and collected in 0.5 min intervals into five 96-deep well plates and stored at −80°C.

Two-dimensional protein map analysis

Two-dimensional protein expression maps of day 6 mice immunized without recall vs with recall, and displaying protein isoelectric point (pI) vs protein hydrophobicity were generated by the ProteoView/DeltaVue software package provided with the PF 2D platform. ProteoVue allows inspection of individual proteome maps by integrating UV peak intensity in the chromatograms with the pI fraction into a band and line format. Ultimately, the map has the appearance of a classical two-dimensional gel with pH gradient on the *x*-axis and hydrophobicity on the *y*-axis. DeltaVue software allows comparison of two maps and tagging a peak of interest.

SDS-PAGE, immunoblotting, and fluorescence staining

Protein samples were heated at 100°C for 10 min in denaturing SDS sample buffer as described before (14). Samples were resolved on 4–15% SDS-PAGE at 150 V for 45–60 min. After electrophoresis, proteins were either stained by Coomassie or transferred onto 0.2 μm nitrocellulose membrane (BioRad) and probed with appropriate Abs. Western blot detection was performed using ECL plus (Amersham Biosciences).

Sample preparation, MALDI TOF, and LC/MS/MS

The PF 2D fractions of interest were lyophilized, resuspended in SDS-PAGE sample buffer, and resolved by 4–15% SDS-PAGE. After electrophoresis, the gel was stained by SYPRO-Ruby (BioRad), and protein detected by fluorescence. Visible bands were excised from the gel and sent to NextGen Sciences, subjected to tryspin digestion on a ProGest workstation, and identified by Matrix-assister laser desorption/ionisation time of flight (MALDI-TOF) and Liquid chromatography-tandem mass spectrometry (LC/MS/MS). MALDI TOF spectra of the sample was acquired in reflectron mode on an Applied Biosystems Voyager DE-STR instrument. Peak list .dat files were created from Data Explorer, part of the ABI Voyager 5.1 software suite. Dat files were converted to .massml files using Proteometrics MoverZ freeware for Windows, version 2001.02.13. Peaks were calibrated against internal tryptic autolysis fragments at 842.51 and 2211.1 within the MoverZ software. The calibrated m/z values were submitted to ProFound version 20040106 under license of Genomic Solutions Inc as part of

the Proteometrics software package for peptide mass fingerprint interrogation. ProFound queried a locally stored copy of the NCBInr database version 072106. The peak selection thresholds were S/N-4; resolution: 6000; intensity of third isotope ≥ ~20% of first isotope; minimum match to ID: 5 peptides. Search Parameters: Miscleavage allowance: 1; reagent used to protect free cysteinyl sulfhydryls: iodoacetamide; partial oxidation of met: allow; labeled masses: monoisotopic; taxonomy search: all kingdoms; enzyme: trypsin; monoisotopic mass threshold: 100 PPM; ignored masses: none.

Database searching: Tandem mass spectra were extracted by Xcalibur (ThermoFisher) rev. 2.0. Charge state deconvolution and deisotoping were not performed. All MS/MS samples were analyzed using Mascot version 1.0 (Matrix Science; version Mascot). Mascot was set up to search the ipi.MOUSE.v3.53_plusREV database (110602 entries) assuming the digestion enzyme trypsin. Database was appended with the common Repository of Adventitious Proteins, or cRAP database. Many of these proteins occur in every protein identification experiment and unless the product ion spectra are accounted for can lead to increased false discovery rate (through being allowed to match to incorrect proteins in a database not containing the cRAP sequences). The cRAP sequences have the SwisProt accession number format; their accession number is also listed as the description. More information on cRAP can be found at http://www.thegpm.org/crap/index.html. Mascot was searched with a fragment ion mass tolerance of 0.50 Da and a parent ion tolerance of 2.0 Da. Iodoacetamide derivative of cysteine was specified in Mascot as a fixed modification. S-carbamoylmethylcysteine cyclization (N terminus) of the n terminus, oxidation of methionine and unknown and acetylation of the n terminus were specified in Mascot as variable modifications.

Criteria for protein identification: Scaffold (version Scaffold_2_02_00, Proteome Software) was used to validate MS/MS based peptide and protein identifications. Peptide identifications were accepted if they could be established at >80.0% probability as specified by the Peptide Prophet algorithm (15). Protein identifications were accepted if they could be established at >90.0% probability and contained at least two identified peptides. Protein probabilities were assigned by the Protein Prophet algorithm (16). Proteins that contained similar peptides and could not be differentiated based on MS/MS analysis alone were grouped to satisfy the principles of parsimony. Mascot scores for the two peptides observed to RKIP were 49 and 78, respectively. Manual inspection of the product ion data supported the reported sequence in MASCOT.

Flow cytometry

RBC depleted spleens and lymph node cells were resuspended with staining buffer (BSS, 3% FBS and 0.1% sodium azide), followed by blocking with a mixture of normal mouse serum, anti-Fc receptor supernatant from the 2.4 G_2 hybridoma (17), and human gamma globulin. Incubation with labeled primary Abs and flow cytometry analysis was conducted as before (18). For intracellular cytokine staining, spleen cells were cultured for 5h with SIINFEKL recall peptide in the presence of BFA, and then stained for TNF-α and IFN-γ as before (19).

In vitro CTL generation assay

CTL were generated from PBMC as described previously (20). In brief, PBMC was isolated from peripheral blood by Ficoll-Hypaque gradient separation method and adherent macrophages were separated and differentiated into dendritic cells (DC). The $CD8^+$ population was isolated from nonadherent peripheral blood lymphocytes using Dynal magnetic bead isolation kit (Dynal). The purity was routinely >90%. The $CD8^+$ cells were cocultured for 10 days with mature autologous DCs pulsed with $MP_{58–66}$ (GILGFVFTL) peptide of influenza A virus.

Human CTL and PBMC assays

Total human PBMC and Flu-specific CTLs were used to assess the effects of locostatin on LPS-induced and Ag-specific cytokine secretion respectively. For PBMC, 3×10^5 cells were cultured in the presence of increasing doses of LPS for 3 h before supernatant collection. For the Ag-specific cytokine secretion assays, 10^4 T2 cells were pulsed for 2 h at 37°C with different doses of $MP_{58–66}$ (GILGFVFTL) peptide and then 10^5 CTLs were added to each well in a 96-well plate. After overnight incubation, supernatant was collected. TNF-α and IFN-γ in supernatant were measured by ELISA kits (R&D Systems).

Results

To elucidate the mechanism by which T cell activation leads to exacerbated production of potentially toxic cytokines, we used an in vivo model developed by our laboratory (7,8). C57BL/6 mice adoptively transferred with CD45.1 congenic TCR transgenic OT-I cells were immunized with a combination of T cell costimulation and TLR3 ligand in the presence of Ag. This protocol induces specific T cell priming and accumulation of effector cells as previously reported (7). To measure the cytokine producing capacity by specific effector T cells, in vivo recall with SIINFEKL peptide was performed 6 days after immunization. Intracellular cytokine staining of $CD8^+$ OT-I cells revealed rapid and robust production of IFN-γ after recall compared with resting cells (no recall) (Fig. 1, *A* and *B*). Concomitantly, abundant amounts of TNF-α were detected in serum as early as 30 min after recall (Fig. 1*C*).

To identify regulators of this vigorous response, resting cells were compared with in vivo recalled cells and analyzed by the PF 2D proteomics platform as described before (9) (Fig. 2*Ai*). PF 2D proteomics enables protein separation by charge followed by reverse-phase chromatography (Fig. 2*Aii*). Overlay of the proteomic maps from resting and recalled samples revealed identical patterns called signatures as illustrated in Fig. 2*B* (*top right*), and differential chromatographic profiles called fingerprints (Fig. 2*B*, *bottom right*). After analysis of proteomic maps obtained from four independent in vivo experiments, we identified a fingerprint at specific coordinates, present in the recall samples and absent or reduced in the resting samples (Fig. 2*B*, *bottom right*). To identify the protein contained in the fingerprint, a third dimension was executed. The fractions of interest from the recalled and resting samples were lyophilized, resolved by SDS-PAGE, and detected by fluorescent dye staining (Fig. 3*A*, *top left*). The 22-kDa band uniquely detected in the recall sample (Fig. 3*A*, *top right*) was removed, digested with trypsin, and RKIP was identified with 40% sequence coverage by MALDI TOF peptide mass fingerprinting (Fig. 3*A*, *bottom table*). RKIP was also identified in a biological replicate by LC/MS/MS with 20% sequence coverage (data not shown). The original search of the LC/MS/MS data was corroborated by a more recent search of the data using updated software tools and a more robust database. Therefore, RKIP was identified twice, first by MALDI-TOF then by LC/MS/MS, in two biological replicates localized at the same position on the proteomic map.

RKIP expression levels are modulated in certain cancers to promote cell invasion (21–23), and RKIP is also induced during DC and macrophage differentiation (24). Nevertheless, in our model we did not detect changes in RKIP expression before or after immunization, nor following recall (Fig. 3*B*, *top left*). We also controlled for RKIP loss during sample preparation because we found comparable expression in the cell lysate samples loaded on the PF 2D platform (Fig. 3*B*, *top right*). Moreover, RKIP expression remained constant during the 3 h recall (Fig. 3*B*, *bottom*). Therefore, the difference of localization of RKIP on the proteomic map is independent of its expression, but likely due to a modification of charge, hydrophobicity, or binding pattern. Most likely, posttranslational modification of RKIP such as phosphorylation (25) or oxidation, as observed by MS sequencing (Fig. 3*A*, *bottom*), may modify RKIP localization on the proteomic map. Alternatively, because RKIP possesses a ligand-binding

pocket and a globular structure that provides surface area for interaction with other proteins (26), our observation may reflect a differential RKIP-protein interaction. In any case, elucidation of this question will require identifying RKIP posttranslational modifications or interactions rather than strategies targeting its expression.

Locostatin is an oxazolidinone derivative known to specifically bind and inhibit RKIP function (13,27). When treated with locostatin, Ag-specific T cells restimulated ex vivo with SIINFEKL peptide drastically reduced their production of both TNF-α and IFN-γ (Fig. 4, *A* and *B*). Culture supernatants obtained from a similar experiment as described in Fig. 4 showed a titratable and general reduction (up to 4 log) of cytokines and chemokines (Supplementary table).[4] Moreover, as shown before in other models (13,27), we did not observe significant toxicity at even the highest dose of locostatin (60 μM). The OT-I cells in dot plots appeared normal, and late application of locostatin ($\geq$60 min) inefficiently blocked cytokine synthesis (Fig. 4, *A* and *C*). Thus, locostatin can induce functional unresponsiveness or anergy defined by the inability to produce many cytokines and chemokines upon TCR triggering.

Because the mechanism by which locostatin promotes T cell anergy is unknown but possibly related to RKIP and its downstream pathways, we hypothesized that locostatin treatment could affect Erk phosphorylation, a pathway uncoupled in anergic T cells (5). Immunoblotting of total splenocytes and lymph node cells recalled ex vivo with SIINFEKL peptide showed a decrease in Erk phosphorylation in the presence of locostatin (Fig. 5*A*). However, we observed the opposite effect in naive spleen cells from OT-I mouse. Locostatin slightly induced ERK phosphorylation with and without SIINFEKL stimulation (Fig. 5*B*). Similarly, locostatin blocked Erk phosphorylation after plate-bound anti-CD3 stimulation of day 6 purified OT-I (Fig. 5*B*). These observations are consistent with the massive decrease of cytokine after locostatin treatment observed in Fig. 4 and supplementary Table I.

Like other pharmacological inhibitors, locostatin also has off target effects including inhibition of aldehyde dehydrogenase 1a1, glutathione *S*-transferase omega 1-1, and prolyl oligopeptidase (13). We tested whether these proteins were the central factor involved in the inhibition of p-Erk, which may explain why our data were different from those reported previously (28,29), albeit in very different model systems, and our data show that none of the three inhibitors impacted p-Erk like locostatin (Fig. 5*D*). Moreover, in the same experiment, we also observed that the Glutathi-one *S*-transferase inhibitor and the prolyl oligopeptidase inhibitor did not block TNF-α and IFN-γ production (data not shown). As expected disulfiram, which is both an aldehyde dehydrogenase inhibitor and importantly a NFκB inhibitor (30,31), inhibited cytokine production (data not shown) but not ERK phosphorylation (Fig. 5*D*).

To validate locostatin as potential therapy for squelching a cytokine storm in vivo, we tested whether locostatin would block the in vivo cytokine synthesis shown earlier (Fig. 1). A single i.p. injection caused profound reduction of TNF-α in mouse serum (Fig. 6*A*). Secondly, in 2 separate experiments, the efficacy of locostatin on human cells was tested with specific CTL against flu Ag and by LPS stimulation of human PBMC. Locostatin drastically inhibited TNF-α production upon restimulation with relevant Ag (Fig. 6*B*, *left*). In the same cells IFN-γ production was affected by 60 μM locostatin (Fig. 6*B*, *right*). Finally, to test the relevance of locostatin for a TLR-based septic shock response in humans, we examined its efficacy on human PBMC treated in vitro with LPS. Although TNF-α production was totally inhibited with as little as 20 μM of locostatin (Fig. 6*C*, *left*), we observed in the same cells a strong inhibition of IFN-γ at 60 μM (Fig. 6*C*, *right*).

[4]The online version of this article contains supplementary material.

Discussion

This is the first study identifying locostatin as an anti-inflammatory compound promoting T cell anergy and TLR inhibition. By comparing the total proteomic profile of resting and reactivated splenocytes, we uncovered RKIP as a differentially regulated protein involved in T effector cell activation status. Because RKIP was equally expressed in resting and recalled cells, we suggest that posttranslational modification like serine phosphorylation (32) could be responsible for differential proteomic mapping. Alternatively, RKIP is known to bind Raf-1 (33), GRK2 (25), MEK (33,34), Erk (34), IKKα and β (35), NIK (35), TAK1 (35), phopshatidylyethanolamine (36), GTP, GDP, small GTP-binding proteins (37), and several serine proteases (38). Therefore, it is conceivable that after immunological recall RKIP remains strongly associated with a ligand, conferring a new biochemical complex that would localize differently on the proteomic map.

Locostatin, an oxazolidinone derivative identified from a small molecule library for its ability to inhibit cell migration (27), specifically and covalently binds RKIP (13). We tested locostatin in an immunological model and observed its potent ability to inhibit the secretion of various cytokines (supplementary Table I). By focusing on specific $CD8^+$ OT-I cells, we found that locostatin is a compound of immunological interest for inhibiting a cytokine storm by promoting T cell anergy and possibly affecting other immunological cells as well.

To explore the mechanism by which locostatin induced T cell anergy, we focused on the known RKIP pathways. RKIP was previously shown to be involved in preventing chromosomal abnormalities (39), preventing metastasis (21,22) and promoting cell-substratum adhesion (40). More relevant to our study is the role of RKIP in the RAF/MEK/Erk and NFκB pathways (35). We uncovered an inhibitory effect of locostatin on Erk phosphorylation, suggesting a specific block in the activation of Erk may have contributed to inhibition of the cytokine storm. In contrast, locostatin has been shown to abrogate RKIP/Raf-1 interaction, resulting in activation of Raf-1 in vitro (27) and in vivo (28), as well as increased Erk phosphorylation in a model of ischemia reperfusion (28). Therefore, it is likely that the decrease in Erk phosphorylation with locostatin treatment in primed lymphocytes is an indirect phenomenon, possibly due to other RKIP-regulated proteins or a feedback loop expressed in lymphocytes. However, locostatin induced Erk phosphorylation during TCR stimulation of naive T cells (Fig. 5*B*) similar to other models (28,29). Our finding of decreased p-Erk during TCR stimulation of effector T cells but increased with naive T cells, is a new result that may be related to the different signaling pathways activated in naive vs effector T cells. Therefore, future studies should test how locostatin cooperates with specific pathways differentially in naive vs effector T cells.

Although the detailed mechanism by which locostatin affects Erk phosphorylation in lymphocytes remains to be determined, a nonacylated analog of locostatin appears to bind to the phosphatidylethanolamine-binding pocket of RKIP (41). Off target effects of locostatin have also been shown in previous studies (13,41). In our model, blockage of the four known locostatin targets indicated that only locostatin could affect Erk phosphorylation. This is an important aspect to understand when bringing locostatin forward into a clinical setting, which will involve careful delineation of toxicity, pharmacological dose, and delivery.

The validation of locostatin as an efficient countermeasure to TNF-α production in vivo (Fig. 6*A*) suggests it may be applicable for the treatment of inflammatory diseases in which this cytokine causes toxicity. Blocking TNF-α at the source of production would complement an already existing therapy for rheumatoid arthritis (42,43). A similar strategy could be applied for the treatment of psoriatic arthritis, inflammatory bowel disease, and multiple sclerosis. Interestingly, locostatin has all the advantages recently listed for the generation of new

compounds to be used in anti-TNF-α therapy (44). Locostatin is a molecule easy to manufacture, theoretically too small to be immunogenic, specific for a known signaling pathway, and can be used in combination with other anti-inflammatory modalities. Moreover, locostatin does not inhibit the growth of Gram-positive or Gram-negative bacteria (27) and thus should be amendable to oral delivery without side effects against the gut flora. The efficacy of locostatin on human anti-flu CTL suggests it could also be used in overzealous pathological responses like the 1918 Spanish influenza pandemic, which was particularly deadly for young adults between the age of 18–30 years old, possibly due to a hyper inflammatory response (45). Another application is illustrated by its ability to block TNF-α production from human PBMCs stimulated with LPS (Fig. 6*C*). Among the various strategies proposed to treat sepsis, the generation of therapies that specifically disrupt LPS signaling are favored (46). Therefore, locostatin is an important compound for further investigation in the treatment of sepsis. We propose that locostatin would be beneficial in the treatment of autoimmune diseases such as multiple sclerosis, arthritis, and systemic lupus erythematosus by restoring a natural cytokine balance.

Supplementary Material

Refer to Web version on PubMed Central for supplementary material.

References

1. Bretscher P, Cohn M. A theory of self-nonself discrimination. Science 1970;169:1042–1049. [PubMed: 4194660]
2. Jenkins MK, Schwartz RH. Antigen presentation by chemically modified splenocytes induces antigen-specific T cell unresponsiveness in vitro and in vivo. J Exp Med 1987;165:302–319. [PubMed: 3029267]
3. Vignali DA, Collison LW, Workman CJ. How regulatory T cells work. Nat Rev Immunol 2008;8:523–532. [PubMed: 18566595]
4. Pandiyan P, Zheng L, Ishihara S, Reed J, Lenardo MJ. $CD4^+CD25^+Foxp3^+$ regulatory T cells induce cytokine deprivation-mediated apoptosis of effector $CD4^+$ T cells. Nat Immunol 2007;8:1353–1362. [PubMed: 17982458]
5. Li W, Whaley CD, Mondino A, Mueller DL. Blocked signal transduction to the ERK and JNK protein kinases in anergic $CD4^+$ T cells. Science 1996;271:1272–1276. [PubMed: 8638107]
6. Powell JD, Zheng Y. Dissecting the mechanism of T-cell anergy with immunophilin ligands. Curr Opin Investig Drugs 2006;7:1002–1007.
7. Myers L, Takahashi C, Mittler RS, Rossi RJ, Vella AT. Effector CD8 T cells possess suppressor function after 4-1BB and Toll-like receptor triggering. Proc Natl Acad Sci USA 2003;100:5348–5353. [PubMed: 12695569]
8. Myers LM, Vella AT. Interfacing T-cell effector and regulatory function through CD137 (4-1BB) co-stimulation. Trends Immunol 2005;26:440–446. [PubMed: 15979409]
9. Nakanishi M, Menoret A, Giardina GS, Godman C, Vella AT, Rosenberg DW. Utilizing endoscopic technology to reveal real-time proteomic alterations in response to chemoprevention. Proteomics Clin Appl 2007;1:1660–1666.
10. Hogquist KA, Jameson SC, Heath WR, Howard JL, Bevan MJ, Carbone FR. T cell receptor antagonist peptides induce positive selection. Cell 1994;76:17–27. [PubMed: 8287475]
11. Shuford WW, Klussman K, Tritchler DD, Loo DT, Chalupny J, Siadak AW, Brown TJ, Emswiler J, Raecho H, Larsen CP, et al. 4-1BB costimulatory signals preferentially induce $CD8^+$ T cell proliferation and lead to the amplification in vivo of cytotoxic T cell responses. J Exp Med 1997;186:47–55. [PubMed: 9206996]
12. Moffit JS, Boekelheide K, Sedivy JM, Klysik J. Mice lacking Raf kinase inhibitor protein-1 (RKIP-1) have altered sperm capacitation and reduced reproduction rates with a normal response to testicular injury. J Androl 2007;28:883–890. [PubMed: 17554109]

13. Zhu S, Mc Henry KT, Lane WS, Fenteany G. A chemical inhibitor reveals the role of Raf kinase inhibitor protein in cell migration. Chem Biol 2005;12:981–991. [PubMed: 16183022]
14. Menoret A, Bell G. Purification of multiple heat shock proteins from a single tumor sample. J Immunol Methods 2000;237:119–130. [PubMed: 10725457]
15. Keller A, Nesvizhskii AI, Kolker E, Aebersold R. Empirical statistical model to estimate the accuracy of peptide identifications made by MS/MS and database search. Anal Chem 2002;74:5383–5392. [PubMed: 12403597]
16. Nesvizhskii AI, Keller A, Kolker E, Aebersold R. A statistical model for identifying proteins by tandem mass spectrometry. Anal Chem 2003;75:4646–4658. [PubMed: 14632076]
17. Unkeless JC. Characterization of a monoclonal antibody directed against mouse macrophage and lymphocyte Fc receptors. J Exp Med 1979;150:580–596. [PubMed: 90108]
18. Menoret A, Myers LM, Lee SJ, Mittler RS, Rossi RJ, Vella AT. TGFβ protein processing and activity through TCR triggering of primary $CD8^+$ T regulatory cells. J Immunol 2006;177:6091–6097. [PubMed: 17056535]
19. McAleer JP, Zammit DJ, Lefrancois L, Rossi RJ, Vella AT. The lipopolysaccharide adjuvant effect on T cells relies on nonoverlapping contributions from the MyD88 pathway and $CD11c^+$ cells. J Immunol 2007;179:6524–6535. [PubMed: 17982041]
20. Mehrotra S, Chhabra A, Chattopadhyay S, Dorsky DI, Chakraborty NG, Mukherji B. Rescuing melanoma epitope-specific cytolytic T lymphocytes from activation-induced cell death, by SP600125, an inhibitor of JNK: implications in cancer immunotherapy. J Immunol 2004;173:6017–6024. [PubMed: 15528336]
21. Fu Z, Kitagawa Y, Shen R, Shah R, Mehra R, Rhodes D, Keller PJ, Mizokami A, Dunn R, Chinnaiyan AM, et al. Metastasis suppressor gene Raf kinase inhibitor protein (RKIP) is a novel prognostic marker in prostate cancer. Prostate 2006;66:248–256. [PubMed: 16175585]
22. Hagan S, Al-Mulla F, Mallon E, Oien K, Ferrier R, Gusterson B, Garcia JJ, Kolch W. Reduction of Raf-1 kinase inhibitor protein expression correlates with breast cancer metastasis. Clin Cancer Res 2005;11:7392–7397. [PubMed: 16243812]
23. Schuierer MM, Bataille F, Hagan S, Kolch W, Bosserhoff AK. Reduction in Raf kinase inhibitor protein expression is associated with increased Ras-extracellular signal-regulated kinase signaling in melanoma cell lines. Cancer Res 2004;64:5186–5192. [PubMed: 15289323]
24. Schuierer MM, Heilmeier U, Boettcher A, Ugocsai P, Bosserhoff AK, Schmitz G, Langmann T. Induction of Raf kinase inhibitor protein contributes to macrophage differentiation. Biochem Biophys Res Commun 2006;342:1083–1087. [PubMed: 16513087]
25. Lorenz K, Lohse MJ, Quitterer U. Protein kinase C switches the Raf kinase inhibitor from Raf-1 to GRK-2. Nature 2003;426:574–579. [PubMed: 14654844]
26. Granovsky AE, Rosner MR. Raf kinase inhibitory protein: a signal transduction modulator and metastasis suppressor. Cell Res 2008;18:452–457. [PubMed: 18379591]
27. Mc Henry KT, Ankala SV, Ghosh AK, Fenteany G. A non-antibacterial oxazolidinone derivative that inhibits epithelial cell sheet migration. Chembiochem 2002;3:1105–1111. [PubMed: 12404636]
28. Guo J, Wu HW, Hu G, Han X, De W, Sun YJ. Sustained activation of Src-family tyrosine kinases by ischemia: a potential mechanism mediating extracellular signal-regulated kinase cascades in hippocampal dentate gyrus. Neuroscience 2006;143:827–836. [PubMed: 17000055]
29. Ma J, Li F, Liu L, Cui D, Wu X, Jiang X, Jiang H. Raf kinase inhibitor protein inhibits cell proliferation but promotes cell migration in rat hepatic stellate cells. Liver Int 2009;29:567–574. [PubMed: 19323783]
30. Lovborg H, Oberg F, Rickardson L, Gullbo J, Nygren P, Larsson R. Inhibition of proteasome activity, nuclear factor-κB translocation and cell survival by the antialcoholism drug disulfiram. Int J Cancer 2006;118:1577–1580. [PubMed: 16206267]
31. Wang W, McLeod HL, Cassidy J. Disulfiram-mediated inhibition of NF-κB activity enhances cytotoxicity of 5-fluorouracil in human colorectal cancer cell lines. Int J Cancer 2003;104:504–511. [PubMed: 12584750]
32. Corbit KC, Trakul N, Eves EM, Diaz B, Marshall M, Rosner MR. Activation of Raf-1 signaling by protein kinase C through a mechanism involving Raf kinase inhibitory protein. J Biol Chem 2003;278:13061–13068. [PubMed: 12551925]

33. Yeung K, Seitz T, Li S, Janosch P, McFerran B, Kaiser C, Fee F, Katsanakis KD, Rose DW, Mischak H, Sedivy JM, Kolch W. Suppression of Raf-1 kinase activity and MAP kinase signalling by RKIP. Nature 1999;401:173–177. [PubMed: 10490027]
34. Yeung K, Janosch P, McFerran B, Rose DW, Mischak H, Sedivy JM, Kolch W. Mechanism of suppression of the Raf/MEK/extracellular signal-regulated kinase pathway by the raf kinase inhibitor protein. Mol Cell Biol 2000;20:3079–3085. [PubMed: 10757792]
35. Yeung KC, Rose DW, Dhillon AS, Yaros D, Gustafsson M, Chatterjee D, McFerran B, Wyche J, Kolch W, Sedivy JM. Raf kinase inhibitor protein interacts with NF-κB-inducing kinase and TAK1 and inhibits NF-κB activation. Mol Cell Biol 2001;21:7207–7217. [PubMed: 11585904]
36. Bernier I, Tresca JP, Jolles P. Ligand-binding studies with a 23 kDa protein purified from bovine brain cytosol. Biochim Biophys Acta 1986;871:19–23. [PubMed: 2938633]
37. Bucquoy S, Jolles P, Schoentgen F. Relationships between molecular interactions (nucleotides, lipids and proteins) and structural features of the bovine brain 21-kDa protein. Eur J Biochem 1994;225:1203–1210. [PubMed: 7957211]
38. Hengst U, Albrecht H, Hess D, Monard D. The phosphatidylethanolamine-binding protein is the prototype of a novel family of serine protease inhibitors. J Biol Chem 2001;276:535–540. [PubMed: 11034991]
39. Eves EM, Shapiro P, Naik K, Klein UR, Trakul N, Rosner MR. Raf kinase inhibitory protein regulates aurora B kinase and the spindle checkpoint. Mol Cell 2006;23:561–574. [PubMed: 16916643]
40. Mc Henry KT, Montesano R, Zhu S, Beshir AB, Tang HH, Yeung KC, Fenteany G. Raf kinase inhibitor protein positively regulates cell-substratum adhesion while negatively regulating cell-cell adhesion. J Cell Biochem 2008;103:972–985. [PubMed: 17668446]
41. Shemon AN, Eves EM, Clark MC, Heil G, Granovsky A, Zeng L, Imamoto A, Koide S, Rosner MR. Raf kinase inhibitory protein protects cells against locostatin-mediated inhibition of migration. PLoS One 2009;4:e6028. [PubMed: 19551145]
42. Feldmann M, Maini RN. Lasker Clinical Medical Research Award: TNF defined as a therapeutic target for rheumatoid arthritis and other autoimmune diseases. Nat Med 2003;9:1245–1250. [PubMed: 14520364]
43. Arend WP, Dayer JM. Inhibition of the production and effects of interleukin-1 and tumor necrosis factor α in rheumatoid arthritis. Arthritis Rheum 1995;38:151–160. [PubMed: 7848304]
44. Palladino MA, Bahjat FR, Theodorakis EA, Moldawer LL. Anti-TNF-α therapies: the next generation. Nat Rev Drug Discov 2003;2:736–746. [PubMed: 12951580]
45. Ahmed R, Oldstone MB, Palese P. Protective immunity and susceptibility to infectious diseases: lessons from the 1918 influenza pandemic. Nat Immunol 2007;8:1188–1193. [PubMed: 17952044]
46. Opal SM. The host response to endotoxin, antilipopolysaccharide strategies, and the management of severe sepsis. Int J Med Microbiol 2007;297:365–377. [PubMed: 17452016]

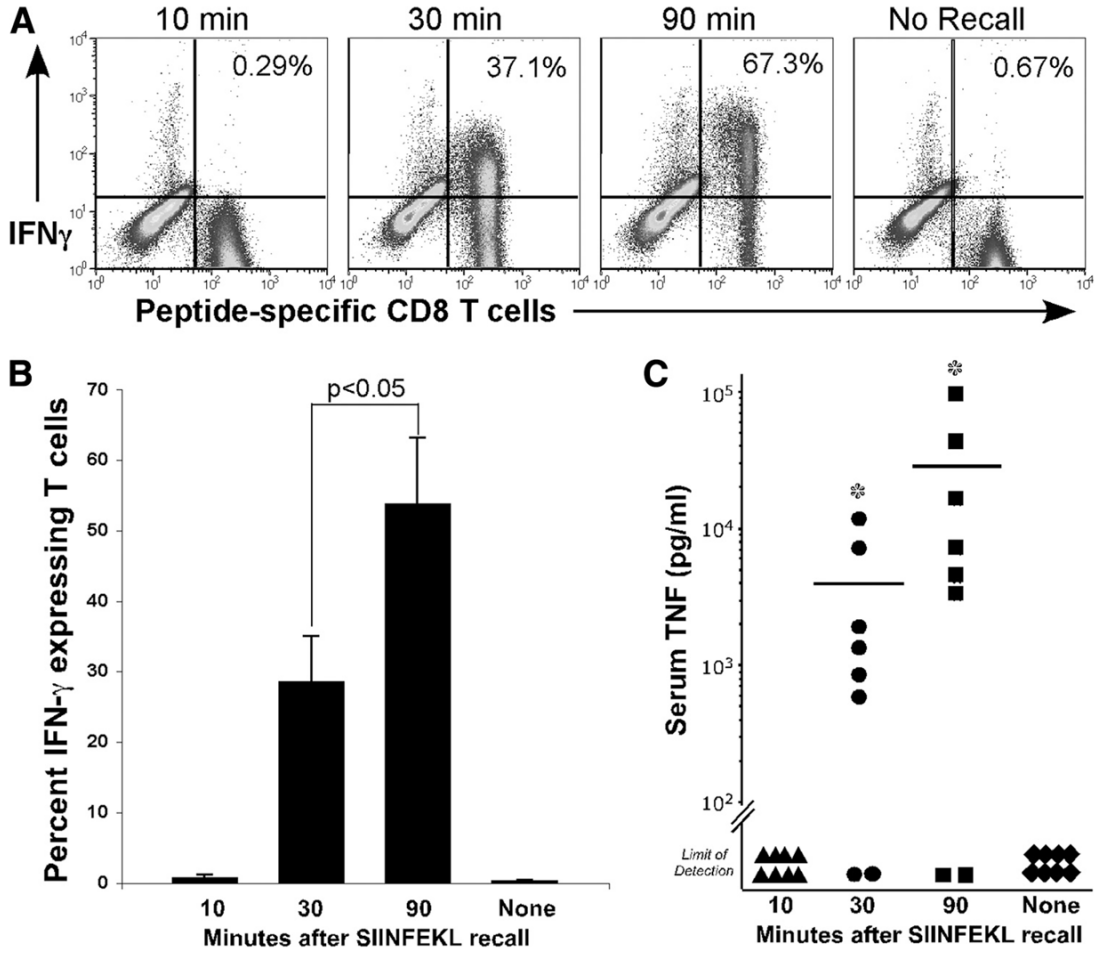

FIGURE 1.

Exacerbated cytokine response after recall of adoptively transferred OT-I cells. *A*, C57BL/6 mice adoptively transferred with 150,000 OT-I cells were immunized with OVA, poly I:C, and anti-4-1BB (CD137) Ab and rested for 6 days. Spleen cells were harvested before (No Recall) and 10–90 min after in vivo recall with 100 μg SIINFEKL peptide. Cells were fixed, permeabilized, and stained for IFN-γ and for the congenic marker CD45.1 (peptide-specific $CD8^+$ T cells). The percentage of OT-I cells ($CD45.1^+$) producing IFN-γ is indicated. *B*, The mean percentage ± SEM of OT-I cells producing IFN-γ from three independent biological replicates is shown. *C*, Sera were obtained and quantified for TNF-α presence by ELISA and shown as individual scatter plots. Because the data were not normally distributed, a Mann-Whitney *U* test was used and the results showed a $p < 0.05$ compared with 10 min or no recall.

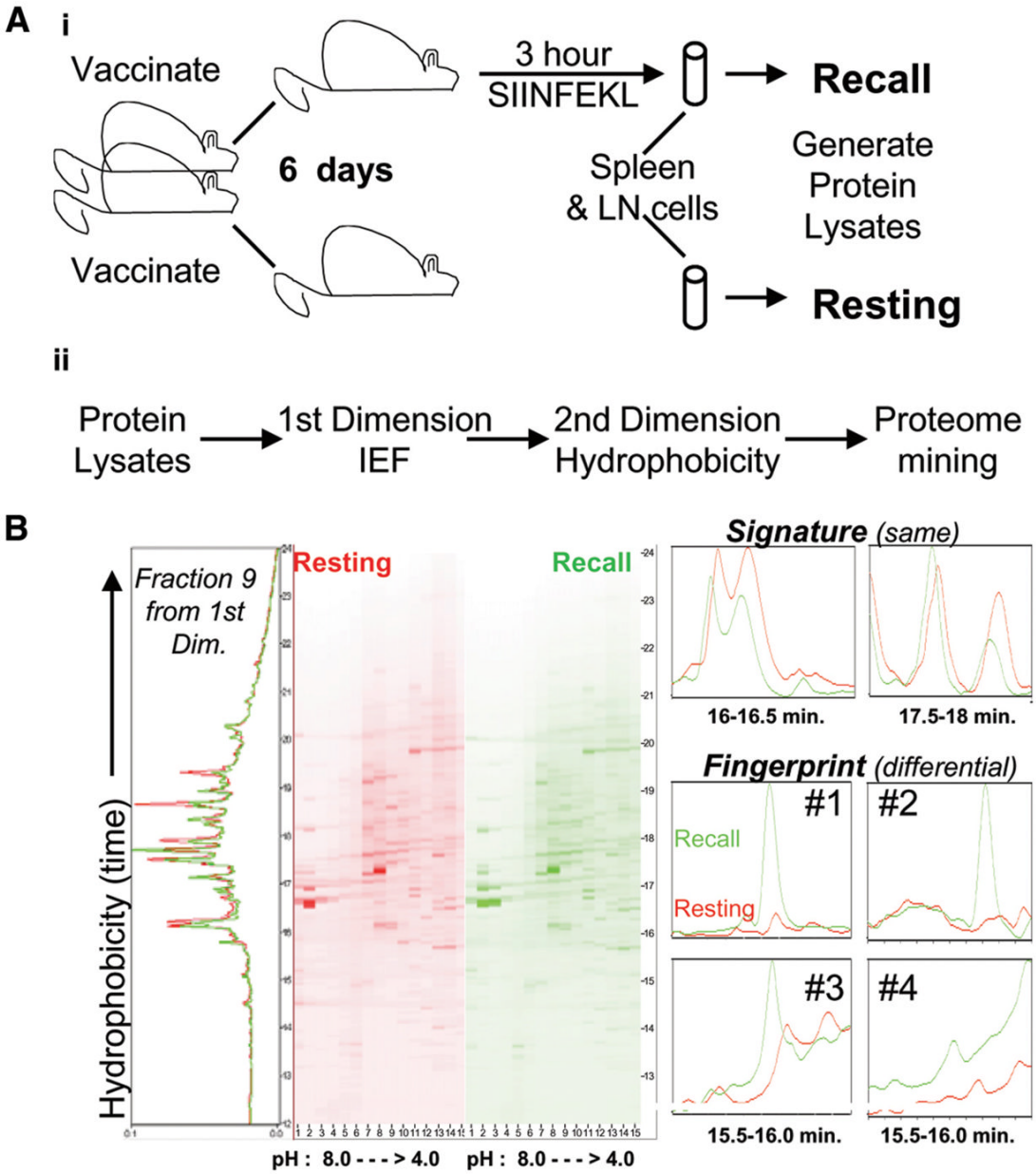

FIGURE 2.

Differential proteomic fingerprint of Resting vs Recall cells. *Ai*, C57BL/6 mice transferred with OT-I cells were immunized as described in legend of Fig. 1 and recalled for 3 h after i.p injection with 100 μg SIINFEKL (Recall), or left untouched (Resting). Splenocytes and lymph node cells were harvested, lysed, and applied to the PF 2D platform. *Aii*, The lysate was processed on a Beckman Coulter ProteomeLab PF 2D platform. The chromatofocusing was performed as linear gradient from ph 8.0 to 4.0. Fractions were collected in 0.3 pH intervals, automatically reinjected for a second dimension on C18 column at 50°C. Two-dimensional protein expression maps displaying protein isoelectric point (pI) vs protein hydrophobicity were generated by Proteo-View/DeltaVue software package. *B*, A comparative two-dimensional map representative of one out four in vivo experiments is shown (*left*). Each experiment identified similar chromatographic profiles we call signatures as well as differential

ones we call finger-prints. In every one of the four experiments (*Right*, no. 1 to 4) we found, at the same precise coordinates on the proteomic maps, a reproducible fingerprint showing a peak present in the recall and absent (or smaller) in the resting sample.

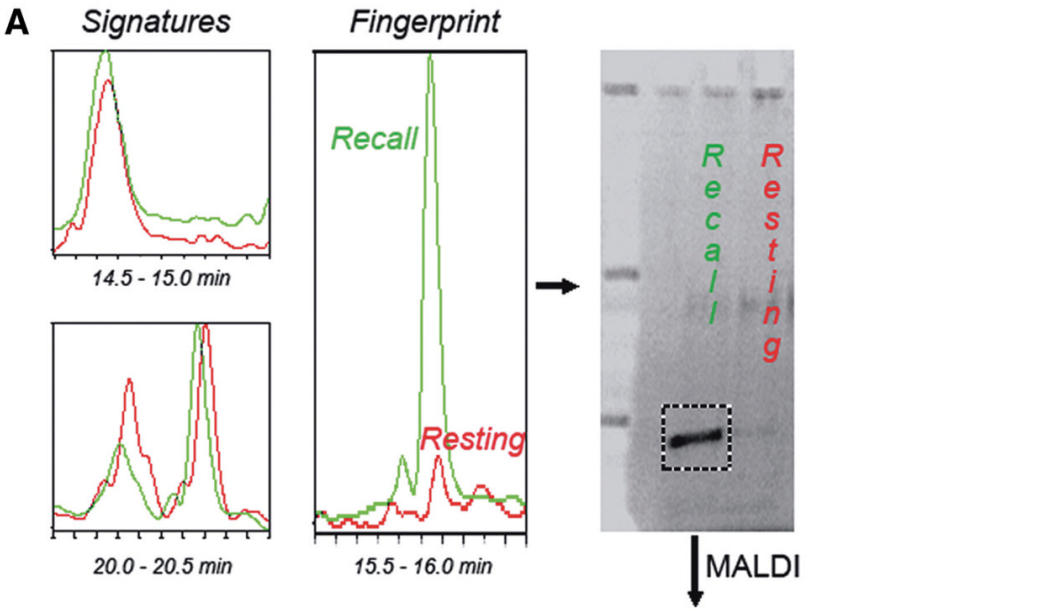

Mass	Start	To	Peptide sequence
925.5	149	155	FKVETFR
1364.6	27	39	VDYAGVTVDELGK
1559.8	63	76	LYTLVLTDPDAPSR
1687.9	63	77	LYTLVLTDPDAPSRK
1757.8	81	93	FREWHHFLVVNMK +1oxidized M
2529.2	94	119	GNDISSGTVLSDYVGSGPPSGTGLHR

Unique peptides identified : 6
% of sequence coverage : 39.6
Accession number : gi|14198222|gb|AAH08169.1
Name: Phosphatidylethanolamine-binding protein; RKIP [Mus musculus]

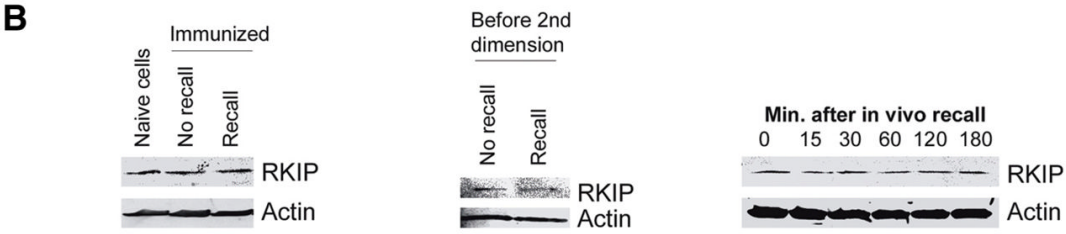

FIGURE 3.

Identification of RKIP as a fingerprint in recall cells. *A*, One second dimension fraction from the recall sample and its corresponding equivalent from the no recall sample were lyophilized and resolved by 4–15% SDS-PAGE. A 22 kDa band, detected by a protein-specific fluorescent dye was cut, digested by trypsin, sequenced by MALDI-TOF. Peptide sequences were searched against using the NCBInr database version 20060804 using the Proteometrics Software Suite and the Profound Search Algorithm. *B*, RKIP expression was assessed by immunobloting of the original sample *(left)*, the cell lysate immediately before loading on the PF 2D (*middle*), and the kinetics of an in vivo recall response (*right*).

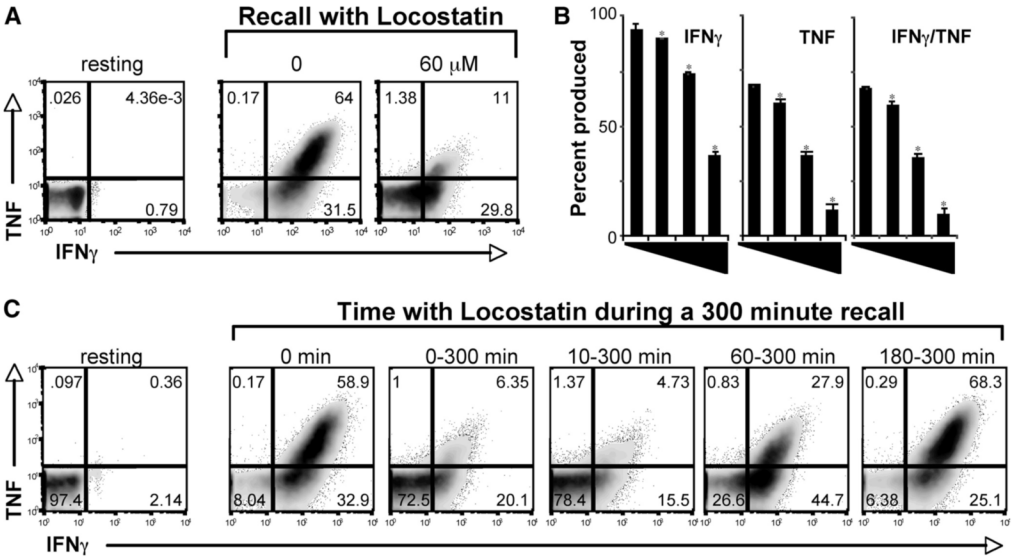

FIGURE 4.

Locostatin, a RKIP-specific compound, induces T cell anergy in vitro. *A*, Splenocytes and LN cells 6 days after immunization as described in legend of Fig. 1 were restimulated in vitro for 5 h with SIINFEKL in the absence or presence of locostatin. Cells were fixed, permeabilized, and stained for IFN-γ, TNF-α and the congenic marker CD45.1. The percentage CD45.1$^+$-gated cells producing IFN-γ and TNF-α is indicated. *B*, The percentage ± SEM of OT-I cells (CD45.1$^+$) producing IFN-γ and TNF-α from five independent experiments (n = 16) is shown for four incremental doses of locostatin: 0 μM, 6.7 μM, 20 μM, and 60 μM. *C*, Inhibition of cytokine secretion was tested by adding the 60 μM of locostatin at 0, 10, 60, and 180 min during a 300 min SIINFEKL restimulation. The percentage CD45.1$^+$-gated cells producing IFN-γ and TNF-α is representative of three independent experiments (n = 14).

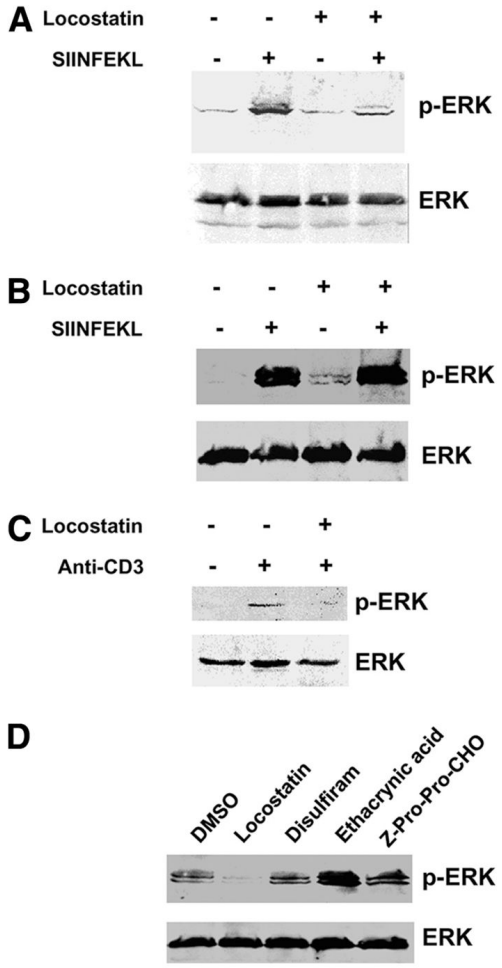

FIGURE 5.

Locostatin inhibits the Erk pathway. *A*, Splenocytes and LN cells 6 days after immunization as described in legend of Fig. 1 were tested for activation of the Erk pathway. Representative Western blots from five independent biological replicates are shown. Cells were preincubated with 60 μM locostatin for 1 h followed by restimulation with/without SIINFEKL for 1 h. Cell lysates were resolved by 4–15% gradient SDS-PAGE under reducing and denaturing conditions, transferred to nitrocellulose membrane and probed with the indicated primary Ab as described in the *Materials and Methods* section. *B*, In three separate experiments, splenocytes and LN cells from naive $Rag^{-/-}$ OT-I mouse were treated with locostatin and analyzed as described in *A. C*, OT-I cells, purified from splenocytes and LN cells 6 days after immunization were plated on plate-bound CD3 for 10 min in presence or absence of 60 μM locostatin. Cell lysates were obtained and processed as described in *A. D*, Splenocytes and LN cells 6 days after immunization, in one experiment ($n = 2$), were preincubated with DMSO or 100 μM locostatin (RKIP inhibitor), 100 μM disulfiram (aldehyde dehydrogenase 1A1 and NFκB inhibitor), 100 μM ethacrynic acid (glutathione *S*-transferase inhibitor), 100 μM Z-Pro-Pro-CHO (prolyl oligopeptidase inhibitor) for 20 min. followed by restimulation with SIINFEKL for 1 h. Cell lysates were obtained and processed as described in *A.*

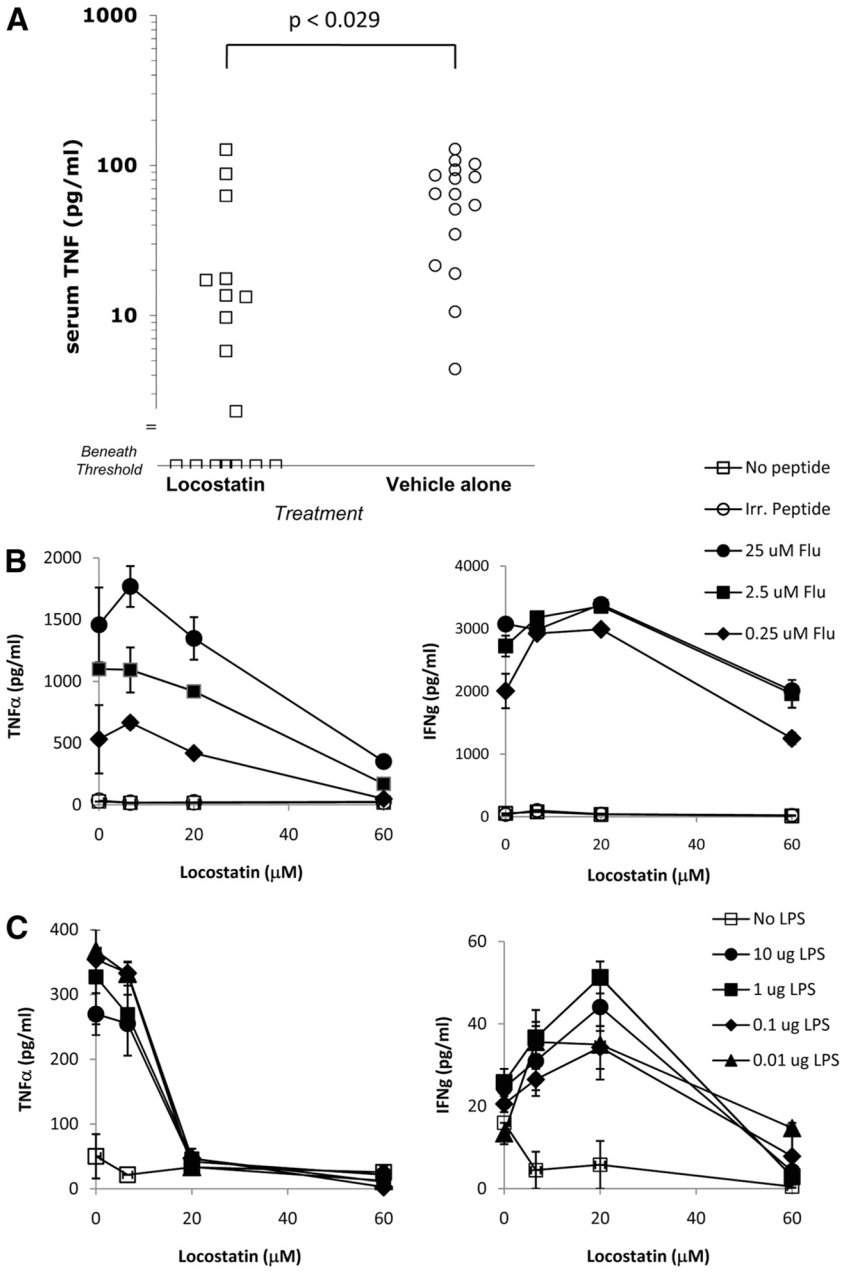

FIGURE 6.

Locostatin inhibit exacerbated TNF-α secretion. *A*, Mice immunized as described in legend of Fig. 1 were injected i.p. with 100 μg of locostatin or vehicle 15 min before i.p. injection with 100 μg of SIINFEKL. A summary of three independent experiments is shown. The mice were bled 1 h later; sera were tested for TNF-α presence by ELISA (pg/ml) and shown as individual scatter plots. *B*, In a complementary experiment, human anti-flu CTL were stimulated for 16 h with increasing doses of cognate peptide in the presence of locostatin. TNF-α and IFN-γ release was measured by ELISA. *C*, Human PBMC were stimulated for 3 h with increasing doses of LPS in the presence of locostatin. TNF-α and IFN-γ release was measured by ELISA.